NASA TECHNICAL NOTE

NASA TN D-2124

NASA TN D-2124

TWO-DIMENSIONAL GRAY-GAS RADIANT HEAT TRANSFER IN A COAXIAL-FLOW GASEOUS REACTOR

by Robert G. Ragsdale and Thomas H. Einstein

Lewis Research Center
Cleveland, Ohio

NATIONAL AERONAUTICS AND SPACE ADMINISTRATION • WASHINGTON, D. C. • FEBRUARY 1964

TWO-DIMENSIONAL GRAY-GAS RADIANT HEAT TRANSFER IN A COAXIAL-FLOW GASEOUS REACTOR

By Robert G. Ragsdale and Thomas H. Einstein

Lewis Research Center
Cleveland, Ohio

NATIONAL AERONAUTICS AND SPACE ADMINISTRATION

For sale by the Office of Technical Services, Department of Commerce,
Washington, D.C. 20230 -- Price $0.75

TWO-DIMENSIONAL GRAY-GAS RADIANT HEAT TRANSFER IN A COAXIAL-FLOW GASEOUS REACTOR

SUMMARY

A two-dimensional radiation heat-transfer analysis was applied to a cylindrical system of coaxially flowing gray gases (constant absorption coefficient) in which the inner stream contains a radially uniform distribution of volumetric heat sources. For slug-flow velocity profiles in both streams, the following conditions were selected: (1) a cavity diameter of 10 feet, (2) cavity lengths of 10, 15, and 20 feet, (3) a heat-generating-core diameter of 2 feet, (4) propellant flow rates up to 33 pounds per second, (5) propellant- to fuel-flow-rate ratios from 24 to 240, (6) an inlet gas temperature of 5000° R, and (7) outlet gas temperatures varying from 7000° to 12,200° R. Radiative end losses were accounted for by assuming the inlet end of the reactor to be at the inlet gas temperature, and the outlet gas end to be at the cylinder wall temperature. Both end surfaces were assumed to be black and porous to the flow.

The absorption coefficient, reactor length, and flow parameters were varied over a range of conditions. Based on these assumptions, the following conclusions were reached. For a 10-foot-diameter reactor and an absorption coefficient of 2 per foot, the heat load on the channel wall was less than 1 percent of the generated power, and the maximum wall heat flux was 12 Btu per second per square inch. The temperature of the heat-generating core is relatively constant over the length of the reactor. Wall heat flux is not significantly affected by the core velocity. From the standpoint of radiant heat transfer, for any given reactor diameter, a small value of cavity length to diameter ratio is desirable for gaseous-reactor application. The heat radiated to the reactor wall comes primarily from the hydrogen immediately adjacent to it. Therefore, the wall heat flux is strongly affected by the propellant (outer stream) flow rate and absorption coefficient and by channel dimensions, but it is not directly affected by changing conditions in the central core itself.

INTRODUCTION

The containment of high-temperature propellants in nuclear and other advanced rocket systems necessitates the consideration of heat transfer by thermal radiation. This will become increasingly true as higher temperature systems are contemplated. Arc jets and plasma flow also fall within this area of interest.

While radiative heat transfer is important in these general systems, it is

especially so for certain gaseous-reactor concepts proposed for nuclear rocket propulsion. In a coaxial-flow (ref. 1) or plasma-core (ref. 2) gaseous-reactor system, for example, heat transfer from a fissioning core to the surrounding hydrogen propellant must be accomplished almost entirely by thermal radiation. Such a requirement will exist for any gaseous-reactor scheme in which the propellant and gaseous nuclear fuel are in separate regions. Even if the propellant and fuel are intimately mixed, radiative heat transfer to the enclosing walls must be considered (ref. 3).

A coaxial-flow gaseous reactor is illustrated in figure 1(a). A central core of low-velocity fissionable gas flows parallel to an annular high-velocity stream of hydrogen propellant. As the gases flow coaxially through an externally moderated cavity, fission heat is released in the core region and radiated and conducted to the surrounding propellant. The heated gases are then expanded through an exhaust nozzle to produce thrust.

The success of such a system obviously requires that most of the radiated energy be absorbed by the propellant, rather than by the containing wall. It is equally manifest that the hydrogen, which is transparent at temperatures below approximately $10{,}000^{\circ}$ R, must be seeded with solid particles or other gases to render it absorbent to radiation. Some transmissivity measurements of solid-particle dispersions are reported in reference 4.

With the assumption that the propellant is absorptive, the primary question of interest is the following: What absorption coefficient is required such that only a small fraction, for instance, 1 or 2 percent, of the thermal energy radiated from the fissioning core is transmitted to the wall? Some estimates of radiant wall heating in gaseous reactors have been reported. A one-dimensional analysis is used in reference 5 to compare the spectral distribution reaching the wall with blackbody radiation; the importance of the H^- ion to high-temperature hydrogen radiative characteristics is investigated. Reference 6 presents a one-dimensional transport analysis of high-temperature hydrogen radiative heat transfer for an assumed pressure distribution; spectral absorption coefficients are given for hydrogen and a hydrogen - gray-gas mixture. Both references 5 and 6 utilize an assumed temperature profile in lieu of gas flow, conduction, and internal heat generation.

A two-dimensional radiative heat-transfer analysis is presented in reference 7 for a gray gas flowing through a cylindrical channel of finite length. Internal heat generation in a centrally located cylindrical core is taken into account, and the relative contributions of conductive and radiative heat transfer are evaluated. The analysis is uniquely suited to the situation at hand and has been used herein to investigate the radiative heat-transfer characteristics of a coaxial-flow gaseous reactor.

Because the reactor considered herein is intended as a propulsion device, the values of the parameters were selected with this in mind; some of them were taken as constant. All the calculations are for a 10-foot-diameter cavity, because reactor criticality and pressure requirements dictate that a gaseous reactor be of relatively large dimensions. It is assumed that the solid regions of the reactor will be operated at or near materials limits; both the cavity wall

and the hydrogen propellant entering the cavity are taken to be at 5000° R. The heat-transfer parameter of interest is the fraction of heat generated in the fissioning core that reaches the cylindrical cavity wall. The study reported herein is the effect on this parameter of (1) the gray-gas absorption coefficient (gray is used to mean independent of temperature, wavelength, and species), (2) the propellant flow rate, (3) the propellant- to fuel-flow-rate ratio, (4) the volumetric heat-generation rate, (5) the reactor length, and (6) a linear axial decrease of volumetric heat-generation rate compared with a constant rate. Items (3) and (6) serve to represent the effects of the actual flow situation (ref. 8). In addition to the fraction of the generated heat reaching the cavity wall, the axial variation of local wall heat flux is investigated and discussed.

Though radiant heat transfer is dominant in a coaxial-flow reactor, the analysis also takes into account the effects of heat transfer by thermal conduction. For the case of a transparent gas heated by a hot wall, the present analysis is compared to the rigorous Graetz solution; radial-temperature profiles at various axial positions were computed by both methods.

SYMBOLS

A surface area of elemental gas volume in eq. (1)

Bo Boltzman number, eq. (2)

c_p specific heat

D reactor cavity diameter

dv infinitesimal gas volume in eq. (1)

f gas-gas exchange factor, eq. (1)

G mass flow velocity, for all radial zones when without a subscript

g gas-surface exchange factor, eq. (1)

K absorption coefficient

k thermal conductivity

L reactor cavity length

q total heat-generation rate in core region

q'' heat flux

q''' volumetric heat generation, in all axial zones when without a subscript

R reactor cavity radius

r radial coordinate

T temperature

T^*	dimensionless temperature in eq. (4)
w_p	propellant flow rate
x	axial coordinate
η	conduction-radiation parameter, eq. (3)
σ	Stefan-Boltzmann constant
τ_o	opacity, KD

Subscripts:

gen	generated
p	propellant
s	surface
w	cylinder wall
1	inlet
2	outlet
1,2,3,4,5	radial zones of G
1,2,3,...,10	axial zones of q'''

ANALYSIS

Basic Analysis

A two-dimensional gray-gas analysis of the radiant heat transfer in the model shown in figure 1(b) is presented in detail in reference 7 and will be but briefly reiterated here. A coaxial stream of two gray gases enters the cylinder through one end at a uniform temperature T_1. The radius of the inner stream is 0.2 of that of the outer stream and surrounding cylinder wall. The mass velocity profiles of both streams are radially uniform, but not necessarily equal. The radiation absorption coefficients of both streams are assumed to be equal.

Heat-generating sources are uniformly distributed throughout the inner stream, and the resultant energy is released from this core region primarily by thermal radiation. The outer stream, being absorbent to thermal radiation, is thereby heated as it flows through the cylindrical reactor chamber, and both streams exit at some mixed mean temperature T_2. The radial temperature profile at the reactor exit will generally be nonuniform. The cylinder surface is black and at constant temperature T_w. Radiant interchange with the reactor end faces is represented by a porous (to the flow) surface that is taken to be at T_1 at the inlet end and T_w at the exit. This latter boundary condition is discussed

in the following section (p. 6). Both the end and cylinder wall surfaces are assumed to be black.

The analysis takes into account the following radiant interchanges:

(1) Gas to gas

(2) Gas to end surfaces

(3) Gas to wall

(4) Wall to wall

(5) Wall to end surfaces

(6) End surface to end surface

The effects of flow and radial conduction (axial conduction is neglected) are included in the analysis.

The basic two-dimensional integrodifferential equation is obtained by taking a heat balance on an infinitesimal gas volume dv within the system. The radiative, convective, and conductive heat-loss terms are equated to those representing heat gain due to absorbed radiation from the surrounding gas, absorbed radiation from the pipe wall and end surfaces, and internal heat generation. In that order, the terms are

$$4K\sigma T^4 + Gc_p \frac{\partial T}{\partial x} - \frac{k}{r}\frac{\partial}{\partial r}\left(\frac{\partial T}{\partial r}\right) = K\int\int\int \sigma T^4 f \, dv + K\int\int \sigma T_s^4 g \, dA + q''' \qquad (1)$$

Here the surface temperature T_s is either that of the inlet surface T_1, the outlet surface T_2, or the pipe wall T_w. The exchange factors for gas-gas and gas-surface radiant interchange are f and g, respectively. In general, these exchange factors are functions of the gas absorption coefficient and the channel dimensions; detailed derivations are given in reference 7.

The solution of equation (1) was obtained numerically by considering the system to be composed of 50 zones, 5 radial and 10 axial, as indicated in figure 1(b). Equation (1) is solved by approximating the derivatives by algebraic-difference quotients in terms of gas-zone-center temperatures and the integrals by finite sums that are algebraic functions of the gas-zone-center temperatures. The Newton-Raphson numerical technique is used to solve the resulting system of 50 nonlinear algebraic equations for the 50 gas-zone-center temperatures. The computations are carried out by a program written for the IBM 7090 digital computer. A more detailed treatment of the basic analysis is presented in reference 7.

As indicated in reference 7, the accuracy of the analysis decreases with increasing gas opacity, because this results in progressively less interaction between adjacent zones. Reference 7 suggests, somewhat arbitrarily, an upper limit on zone opacity - the product of zone width and absorption coefficient -

of 1.0. For this opacity, radiation is attenuated to 0.6 of its initial intensity over a linear distance of one-half the zone thickness. The parameter variations reported herein were for a zone opacity of 1.4 (an absorption coefficient of 1.4/ft, a 5-ft-radius cavity, and five radial zones); for this opacity, radiation is attenuated to 0.5 of its initial value in one-half the zone thickness. Thus, an opacity of 1.4 should introduce little additional error, compared with an opacity of 1.0. Further, since the parameter variations are for a constant opacity, the indicated trends should be correct.

In addition to the gray-gas assumption, the absorption coefficients of two streams have been taken equal. The results presented should be relatively unaffected by this assumption when the absorptivity of the outer stream is as large as it is. As the absorptivity of the core changes, the core temperature will change, decreasing with increasing absorption coefficient. The radiated energy will remain the same, however, because the total heat generation is unchanged. Further, a variation of core temperature will not significantly affect the wall heat flux because of the high absorptivity of the intervening gas. Mean outlet temperature is insensitive to core outlet temperature changes because the flow through the heat-generating region is less than 4 percent of the total flow.

Boundary Values and Calculation Procedure

In a gaseous nuclear reactor, both the inlet propellant and the reactor wall will be maintained at maximum temperatures to achieve maximum performance. With one exception, all the results presented in this report are for an initial-gas, inlet- and outlet-surface, and cylinder-wall temperature assumed to be materials limited at 5000° R. The one exception is a series of calculations of the effect of the ratio T_1/T_w. In all cases, the inlet surface temperature is taken to be the same as the inlet gas temperature. The temperature of the exit end surface is in all instances equal to that of the cylinder wall.

It is necessary at this point to discuss the exit surface boundary value of temperature. An inlet surface at the local gas temperature and a cylinder wall at a constant 5000° R are obvious choices that are consistent with the physical realities of the problem under analysis. For the exit end surface, one possible option is to assume that it is at the mean outlet gas temperature. This boundary condition was used in reference 7 and is quite realistic for a situation where the exit end of the cylinder is a porous surface, or where there is no actual surface at all and the gas continues in the flow direction.

Neither of these conditions will exist in a nuclear rocket chamber; there will be an end surface, a nonporous one, and all the gas flow will be directed through a relatively small opening in its center into an exhaust nozzle. With the exception of this central region of hot exhaust, most of the propellant will therefore radiate to an end surface that will be at about the same temperature as the cylinder wall. This condition can most nearly be approximated by the boundary condition used in this report; the exit end surface is assumed to be porous to the flow, but at the same temperature as the cylinder wall. Since, in a reactor, the hot gas in the intermediate region between the core and the channel wall would be deflected toward the exhaust nozzle opening in the exit end and would not pass through the end surface (as it is allowed to in the analysis),

the calculated end wall heat fluxes are higher than would actually be encountered. A more rigorous treatment of radiant heat transfer to the end surface of the reactor and within the exhaust nozzle itself is beyond the scope of this report.

As pointed out in reference 7, the solution of a given flow situation is completely determined by specifying values of the following dimensionless parameters: (1) Boltzmann number Bo, (2) conduction-radiation parameter η, (3) inlet temperature ratio T_1/T_w, (4) temperature rise ratio T_2/T_1, (5) cavity-length to -diameter ratio L/D, and (6) opacity, τ_o. The Boltzmann number and the conduction-radiation parameter are given by

$$Bo = \frac{Gc_p}{\sigma T_w^3} \tag{2}$$

$$\eta = \frac{\frac{k}{D}}{\sigma T_w^3} \tag{3}$$

For assigned values of these parameters, equation (1) can be solved for the 50 gas-zone-center temperature ratios T/T_w. Once the temperature profiles are obtained, the conduction and radiation heat flux to the channel wall zones and the radiative loss to the two end surfaces can be computed.

In the case of a gaseous reactor, certain conditions are relatively invariant; for example, the propellant is hydrogen, so thermal conductivity cannot be varied arbitrarily. Other considerations, such as reactor criticality, hydrodynamic mixing, materials temperature limits, and rocket performance restrict some of the variables to a relatively narrow range of interest. The values chosen for this analysis are listed in the following table:

Assumed conditions	
Reactor cavity diameter, D, ft	10
Fuel diameter, ft	2
Reactor cavity length, L, ft	10 to 20
Thermal conductivity (of both streams), k, Btu/(ft)(sec)($^\circ$F)	0.00161
Inlet gas temperature, T_1, $^\circ$R	5000
Wall temperature, T_w, $^\circ$R	5000
Specific heat (of both streams), c_p, Btu/(lb)($^\circ$F)	12.0

In addition to these values, outer- to inner-stream flow-rate ratios in the range 20 to 1000 are of interest. For most of the calculations presented here, an outer-stream flow rate of 33 pounds per second and a flow-rate ratio of 24 were used. The volumetric heat sources are contained in the central core, of radius ratio 0.2, for all calculations. The volumetric heating rates were chosen to give outlet gas temperatures in the range of interest, 7000° to 15,000° R. The absorption coefficient K was varied to determine its effect on

the fraction of heat generated that reaches the cylinder wall. In general, then, the various parameters (flow rates, outlet temperature, absorption coefficient) were varied to determine their effect on the radiant heat load to the channel wall.

After each of the parameters was varied independently, one case was computed that represents a realistic combination of them all. This case is, of course, somewhat arbitrary, but the values chosen are the best estimate of actual reactor operating conditions based on present information. For this one case, radial temperature profiles and maximum wall heat flux are presented, and the parametric values chosen are discussed.

Finally, the applicability of this analysis to the case of a transparent gas was considered. If a zero absorption coefficient is employed and there is no internal heat generation, the solution obtained should be that for laminar slug flow with a constant wall temperature. This is, of course, the classical Graetz problem, for which the rigorous solution is (ref. 9)

$$T^* = \frac{T - T_l}{T_w - T_l} = 1 - 2 \sum_{n=1}^{\infty} \left[\frac{J_o(\gamma_n R)}{\gamma_n J_1(\gamma_n)} \right] e^{-\gamma_n^2 X} \tag{4}$$

where

$$\gamma_n = \text{roots of } J_o(\gamma) = 0$$

$$R = \frac{r}{r_w}$$

$$X = \frac{\frac{4x}{D}}{RePr}$$

Since there is no internal heat generation, T_w and T_l are not the same value. For an arbitrary case, the temperature profiles obtained by the two methods are compared.

RESULTS AND DISCUSSION

Illustrative Temperature Profiles

Before investigating the effects of various parameters, it will be useful to examine the temperature profiles encountered for typical gaseous-reactor conditions. This reference case was computed for the conditions listed in the previous table and (1) a propellant flow rate of 33 pounds per second, (2) a propellant- to fuel-flow-rate ratio of 24, (3) an absorption coefficient of 1.4 per foot, and (4) a volumetric heat-generation rate of 1.34×10^5 Btu per second per cubic foot. This generation rate, the cavity dimensions listed in the table, and the flow rate in item (1) result in a reactor power of approximately 4210 megawatts and a mean outlet gas temperature of $12{,}200^\circ$ R.

The radial temperature profiles are shown in figure 2(a) at axial positions of 0, 0.5, 2.5, 5, 7.5, and 9.5 feet. The curves illustrate the radial temperature profiles present in such a system. The interesting point here is that the temperatures in the heat-generating core region quickly attain a relatively constant value. This is more clearly shown in figure 2(b), which shows the axial variation of temperature at radii of 0.5 (the radial midpoint of the heat-generating region), 1.5, 2.5, 3.5, and 4.5 feet. The central core temperature rises from its initial value of 5000° R to approximately 22,500° R in the first 2 feet, or 20 percent, of the passage length. The decrease in gas temperature near the exit is due to radiative loss to the end surface, which is at 5000° R. The gas is sufficiently opaque that the gas at a radius of 4.5 feet reaches a temperature of only 8750° R at the exit end. The primary conclusions indicated by figure 2 are that, for these conditions, (1) an assumption of constant core temperature appears reasonable, a fact which greatly facilitates rocket performance calculations, and (2) core temperatures in the range 20,000° to 30,000° R are required to radiate the power levels of interest.

Effect of Propellant Flow Rate

In a rocket application, a case of interest is one of constant propellant enthalpy rise; that is, the heat-generation rate is changed in proportion to the change in mass flow rate. For this condition, the fraction of generated heat reaching the wall decreases with increasing flow rate, as shown in figure 3.

The three solid lines, for absorption coefficients of 1.0, 1.4, and 2.0 per foot, are for the case where the heat-generation rate increases in proportion to the flow rate. Although the heat-generation rate is proportional to the flow rate, the gas outlet temperature does not actually remain constant as the flow rate changes, because the heat transferred to the wall is regarded as a heat loss in these calculations. In other words, a decreasing flow rate is accompanied by an increase in the fractional heat loss to the wall; the corresponding decrease in heat deposited in the flowing gas results in a decreasing outlet gas temperature. For constant outlet temperature, therefore, the heat-generation rate cannot decrease in proportion to the flow rate, and, thus, the heat-loss rate will increase more rapidly with decreasing flow rate. Figure 3 also illustrates the effect of absorption coefficient. For a propellant flow rate of 33 pounds per second, an increase in the absorption coefficient from 1.0 to 2.0 per foot decreases the fraction of generated heat reaching the wall from 8.6 percent to less than 1 percent.

Effect of Annulus- to Core-Flow-Rate Ratio

An inherent operating characteristic of a coaxial-flow reactor is that the flow rate of the heat-generating gas in the inner stream will be from 1/24 to 1/240 of that of the propellant. Calculations were made for ratios of outer- to inner-stream-flow rates varying from 20 to infinity (a stationary inner core), for a propellant flow rate of 33 pounds per second. Figure 4 shows that, as the inner stream slows down relative to the outer stream, the wall heat load increases. The wall heating fraction increases from 4.1 to 5.4 percent as the flow-rate ratio is increased from 24 to infinity, for an absorption coefficient

of 1.4 per foot and an outer-stream-flow rate of 33 pounds per second.

Effect of Axially Dependent Heat Generation

As a direct result of the initial inner-stream velocity deficit and the resultant fluid mixing, an axial decrease of the volumetric heat-generation rate will exist. This condition is approximated in this analysis by considering a heat source strength that linearly decreases in the flow direction. The total heat generation was held constant while various values of the ratio of the first- to last-core-zone heat-generation rate (q_1'''/q_{10}''') were investigated.

The results of this linear variation of volumetric heat source are shown in figure 5. For constant total heat generation, the heat load to the wall increases as the ratio of initial to final heat-generation rate increases. The wall heat load does not increase in direct proportion to q_1'''/q_{10}''', however, and the increase is not large. For a propellant flow rate of 33 pounds per second and an absorption coefficient of 1.4 per foot; a first- to last-zone heat-generation-rate ratio of 2.0 increases the fraction of generated heat reaching the wall from 0.041, for uniform heat generation, to 0.054.

Effect of Volumetric Heat-Generation Rate

Obviously, as reactor power is increased at constant flow rate, the resulting increase in gas temperature will cause an increase in <u>total</u> wall heat flux. Further, because radiant heat transfer to the reactor wall increases as the fourth power of temperature, the <u>fraction</u> of generated heat reaching the wall will also increase.

This effect is shown in figure 6 for cavity lengths of 10, 15, and 20 feet, a flow rate of 33 pounds per second, and an absorption coefficient of 1.4 per foot. For a reactor-channel length of 10 feet, an increase in heat-generation rate from 5000 to 100,000 Btu per second per cubic foot causes the fractional wall heat load to increase from 0.006 to 0.024. As might be expected, for longer passages this increase is much more severe. For a length of 20 feet, this same increase in heat generation increases the fractional wall heat load from 0.013 to well over 0.20 (approx. 0.4, not shown).

Such a comparison must be made with care, however, since a cavity with twice the length requires only approximately one-half the volumetric heat-generation rate to give the same outlet gas temperature. So, a comparison of interest is for the same outlet gas temperature. Dashed lines are shown in figure 6 for constant outlet gas temperature. In figure 6 the wall heating penalty of long cavities is less severe, but is still quite significant at higher exhaust temperatures.

These results indicate that, for exhaust temperatures near 7000° R, a moderate increase in fractional wall heat load results from an increase in cavity length. For an exhaust temperature of 12,200° R, however, an increase in cavity length from 10 to 20 feet results in a rather severe increase in fractional wall heat load from 0.041 to about 0.155.

Effect of Inlet- to Wall-Temperature Ratio

The effect of the inlet-gas- to cylinder-wall-temperature ratio on the fraction of the heat release reaching the wall is shown in figure 7. As the ratio T_1/T_w is decreased, there is a reduction in the fractional wall heat load. Two curves are shown: one is for constant T_1 and the other for constant T_w. The effect of accomplishing a decrease in T_1/T_w by increasing the wall temperature is less pronounced than the effect produced by decreasing the inlet temperature.

Axial Variation of Wall Heat Flux

In addition to the ratio of total wall heat load to the power generated, the local values of wall heat flux are important, since this heat must be removed by forced-convection heat transfer in any steady-state operation. Although the average heat at the cylinder wall surface can be held to about 7 Btu per second per square inch, local values may exceed this by a considerable amount.

The axial variation of local wall heat flux is shown in figure 8. Two curves are shown: one is for uniform volumetric heat generation, and the other is for a linear axial decrease with a first- to last-zone-generation-rate ratio of 2.0. The condition of uniform heat generation is the reference case, the temperature profiles of which are shown in figure 2. The curve for q_1'''/q_{10}''' equal to 2.0 is for the same conditions as for that value in figure 5, which shows that an increase in q_1'''/q_{10}''' from 1.0 to 2.0 resulted in an increase in fractional wall heat load from 0.041 to 0.054. Figure 8 discloses that this increase occurs largely in the downstream portion of the cavity. The mean outlet gas temperature is the same for both cases.

This effect on local heat flux is perhaps opposite to what might be guessed a priori. As a larger fraction of the total reactor power is generated in the inlet region, the heat flux to the wall increases at the outlet end. This reverse effect occurs because most of the radiant heat reaching the wall is emitted by the propellant and not by the heat-generating gas in the core region. So, a shift of heat release to the inlet end causes the high temperatures to progress more rapidly outward through the absorbing propellant in the annular region. Thus, near the outlet of the reactor, the wall "sees" higher temperatures than it did in the other case, although the local heat-generation rate in the core region is less.

This effect is a general characteristic of a highly absorptive gas flowing parallel to a centrally located heat source. The effects observable at the outer boundary are determined by the opacity and flow conditions of the absorbing gas and are not directly influenced by conditions in the central region.

Figure 9 illustrates this phenomenon by showing how the temperature profiles develop as the gas flows through the reactor; the axial temperature variation at various radial positions is shown for q_1'''/q_{10}''' equal to 1.0 and 2.0. The inner core temperatures (at a radius of 0.5 ft) respond quickly to the reactor rear to front shift of power generation and exhibit higher temperatures near the reactor inlet, where q''' is increased, and correspondingly lower temperatures at the outlet, where q''' is decreased. At larger radii, the gas temperature increase

occurs at positions progressively farther along the cavity. Finally, the gas near the reactor wall shows a temperature increase near the reactor outlet. Although the temperature of the central core region is less at the reactor outlet end for the axially varying heat sources, the wall receives radiation from higher temperature propellant and thus experiences an increase in heat flux.

Two conclusions, then, are indicated by the curves in figures 8 and 9. One is that, although the average wall heat flux is less than 4 Btu per second per square inch for uniform axial heat generation, the local heat flux increases rapidly at the outlet end of the reactor and, for the conditions of figure 8, is considerably higher - approximately 11 Btu per second per square inch. The second conclusion is that this situation is not improved by increasing the volumetric heat-generation rate in the inlet portion of the reactor. This, in fact, has the effect of further increasing the peak heat flux at the outlet end of the reactor. Since the reason for this effect is associated with the development of the radial temperature profile in the annular region, improvement is possible by increasing either the propellant opacity or flow rate (this is shown in fig. 3).

GASEOUS-REACTOR OPERATING CONDITIONS - COMBINED CASE

Figures 3 to 9 illustrate the effects of varying the pertinent parameters independently. Based on these trends, a value for each parameter was chosen such that the combination would constitute a reasonable representation of coaxial-flow gaseous-reactor operating conditions. Such a combination is necessarily approximate, and the results obtained point out the direction and magnitude of future problems rather than solve them. Wherever possible, parameter values were chosen to represent rather stringent requirements.

For example, the propellant- to fuel-flow-rate ratio was taken as 2400, though it was only varied from 24 to 240 for the parametric calculations. Similarly, a rather extreme first- to last-zone volumetric heat-generation ratio of 10 (varied from 1.0 to 2.0 in the preceeding calculations) was selected. The numerical values used for this case are given in the following table:

Prescribed gaseous-reactor operating conditions	
Reactor cavity diameter, ft	10
Reactor cavity length, ft	10
Fuel diameter, ft	2
Reactor power level, Mw	3900
Propellant flow rate, w_p, lb/(sec)(sq ft)	33
Propellant- to fuel-flow-rate ratio	2400
First- to last-zone heat-generation ratio	10
Absorption coefficient, K, ft^{-1}	2.0
Wall temperature, T_w, ^oR	5000
Propellant inlet temperature, ^oR	4750
Propellant mean outlet temperature, ^oR	12,200

The radial temperature profiles at axial positions of 0, 0.5, 5.5, and

9.5 feet are shown in figure 10. With an initial heat-generation rate that is ten times the final rate, the fuel-region temperature rises to a near-maximum value of 26,000° R at a distance of only 0.5 foot into the reactor. At the reactor outlet, this core temperature has decreased to 18,000° R. For this case, the average heat load to the reactor wall is less than 1 percent of the reactor power. The maximum heat flux to the wall occurs at the outlet end of the reactor and is 12.2 Btu per second per square inch.

One approximation involved in this calculation is that the heat sources remain confined to a cylindrical region of constant radius in their passage through the reactor. In actual operation, turbulent mixing and diffusion could cause some fuel to move radially outward; however, this would not necessarily result in any great change in temperature profiles and heat flux at or near the cylinder wall. The reason for this is that the absorption coefficient was taken as 2.0 per foot; in a gas of such opacity, radiation is attenuated to less than 2 percent of its initial intensity in a linear distance of 2 feet.

The general conclusion indicated by this calculation is that, for a reactor diameter of 10 feet, a gray-gas absorption coefficient of 2.0 per foot is sufficient to prevent excessive wall heating in a coaxial-flow reactor for mean propellant exhaust temperatures up to 12,200° R.

COMPARISON OF THIS ANALYSIS WITH GRAETZ SOLUTION

Though the opacities of interest for gaseous-reactor conditions are such that radiation is dominant,[1] the accuracy of the conductive contribution can be easily checked by investigating the situation for a completely transparent gas. For zero absorptivity, this analysis can be used to predict developing temperature profiles for laminar slug flow with constant wall temperature and constant properties. If such a solution is of reasonable accuracy, this analysis can be used to predict laminar heat transfer for gases of very low opacity. This situation could exist for transparent gases seeded with small quantities of carbon dust, carbon dioxide, or water vapor.

For an arbitrarily chosen case, radial temperature profiles were calculated by the method of this analysis and compared with the rigorous Graetz solution. Dimensionless temperature profiles obtained by both methods are shown in figure 11. Near the inlet end, where large temperature gradients exist at the wall, the results of this analysis deviate somewhat from the Graetz solution. At an axial position X/L of 0.35 the agreement is good. At the outlet end, the two methods predict temperature profiles that differ by less than 1 percent. For the case illustrated, the mean outlet temperature calculated from the Graetz profiles for a wall temperature of 1000° R would be 915° R. The profiles of this analysis give an outlet temperature of 914° R. This indicates that the method used herein accurately accounts for laminar conduction heat transfer and can be used to predict laminar heat transfer from high-temperature passages to flowing gray gases of low opacity.

---

[1]For the numerical values of this report, the conduction-radiation parameter η is 0.0026. Reference 7 has shown that conduction effects are negligible for $\eta < 0.05$.

SUMMARY OF RESULTS

A study of the radiative heat-transfer characteristics of a coaxial-flow gaseous reactor was made with a two-dimensional gray-gas analysis. Effects of flow and conduction were accounted for, and nuclear heat generation was represented by volumetric heat sources located in a cylindrical core region. The effects of reactor power level, absorption coefficient, propellant- to fuel flow-rate ratio, axially decreasing heat-generation rate, and inlet gas and cylinder wall temperatures were investigated. The effects of these parametric variations were given in terms of the fraction of heat release reaching the reactor wall, local heat fluxes, and temperature profiles.

From the parameter variations investigated, a case was chosen to represent typical gaseous-reactor conditions. Though reactor lengths of 10, 15, and 20 feet were considered, most of the computations were for a reactor cavity length of 10 feet. All calculations were for a reactor cavity diameter of 10 feet, and a fuel diameter of 2 feet. The following statements summarize the results of this study:

1. For a mean propellant exhaust temperature of 12,200° R and other parametric values estimated to be representative of coaxial-flow operating conditions, an absorption coefficient of 2.0 per foot yields a wall heat load of less than 1 percent of the heat generated, and a maximum wall heat flux of 12 Btu per second per square inch.

2. The temperature of the heat-generating core rapidly attains a near-maximum value and is relatively constant throughout the length of the reactor.

3. For a propellant flow rate of 33 pounds per second and an absorption coefficient of 1.4 per foot, a volumetric heat-generation rate that decreases linearly in the axial direction to a final value that is one-half of the initial value results in 5.4 percent of the generated heat reaching the wall compared with 4.1 percent for an axially constant heat generation rate.

4. For an absorption coefficient of 1.4 per foot, as the flow rate of the core region is reduced and the propellant flow rate is held constant at 33 pounds per second, the heat load to the wall increases slightly, from an initial value of 4.1 percent of the total heat release up to a maximum value of 5.4 percent for a stationary inner core.

5. For a propellant flow rate of 33 pounds per second, an absorption coefficient of 1.4 per foot, and a constant outlet temperature of 12,200° R, an increase in reactor length from 10 to 20 feet increases the fractional wall heat load from 0.041 to about 0.155, or 4.1 to 15 percent. This illustrates how heat-transfer considerations will dictate short reactors.

6. For other conditions held constant, either an increase in wall temperature or a decrease in inlet propellant temperature decreases the wall heat load, with the latter being more effective.

7. Because a highly absorbing gas is under consideration, the wall heat flux is primarily affected by conditions near the wall such as propellant temperature,

opacity, and flow rate, and is not directly influenced by changing conditions in the central heat-generating core.

8. For the case of a transparent gas, temperature profiles obtained by the method used in this report are in good agreement with results given by the Graetz solution for laminar heat transfer.

CONCLUDING REMARKS

A number of approximations and assumptions, both expressed and implied, arose throughout this report. They are gathered together here for classification and discussion.

While it is impossible to prefix every conclusive statement with all the premises from which it flows, it is obvious that the results of this study are valid only within the range of assumptions necessary to obtain them. There are two primary restrictive conditions, namely, (1) both the propellant and the fuel are "gray" gases (constant absorption coefficient, independent of temperature and wavelength) and (2) the heat-transfer characteristics of a gaseous reactor can be calculated independent of fluid mechanical and nuclear characteristics.

The gray-gas assumption, though certainly inappropriate for hydrogen gas, is not as serious as it might seem. Since hydrogen is transparent below approximately 10,000° R, it will have to be seeded with another material, or materials, to induce opacity. The grayness or nongrayness of importance is, therefore, that of the seed material to be used. Solid particles and other gases are obviously choices. One possibility, carbon particles, has been shown (in ref. 4) to be relatively gray over the wavelength range of interest. So, it is entirely possible that hydrogen, appropriately seeded, will exhibit properties that are reasonably gray. Even if this is not entirely true, many of the general trends indicated in this report will still apply.

The results of this study indicate that a more rigorous accounting of fluid mechanical and nucleonic conditions will not significantly alter the heat-transfer results. The primary flow simplification is the assumption that the inner stream is not accelerated by the faster moving outer stream and does not diffuse radially into it. From a criticality viewpoint, the situation has been simplified by assuming no radial variation of volumetric heat-generation rate, which implies that there is no neutron flux depression in the high-density fuel core. In short, both assumptions influence the fissioning core - its velocity and source strength distributions. This should not have any major effect on the heat-transfer results, since it has been shown that the propellant flow rate and opacity, not the core conditions, govern the heat transfer to the cavity wall.

It is also of interest to consider the propellant opacity requirement indicated in this report; an absorption coefficient of 2.0 per foot has been shown to be necessary. Based on the results of reference 4, this opacity is attainable with about 0.2 weight percent of 0.5-micron-diameter carbon particles in hydrogen gas at 5000 pounds per square inch absolute and 5000° R. This is not to say that carbon seeding is the answer, but rather that it is one possible candidate and that more information is needed on hydrogen-seed-particle heat transfer, chemical

interaction, and optical properties of the species that will be present in the range 7000° to 10,000° R.

In summary, then, this study has shown that certain coaxial-flow gaseous-reactor characteristics do not appear to give rise to any insurmountable problems and that, although core temperatures of 25,000° R will exist, radiative wall heating is effectively reduced by an intervening opaque gas. It has also been demonstrated that two-dimensional characteristics are present and must be considered, for example, axial variations of wall heat flux. To more nearly approach the actual situation will require a two-dimensional analysis incorporating optical properties of real gases and seed materials and, finally, a coupling of fluid mechanical, nucleonic, and radiative heat-transfer analyses.

Lewis Research Center
National Aeronautics and Space Administration
Cleveland, Ohio, October 28, 1963

REFERENCES

1. Rom, Frank E., and Ragsdale, Robert G.: Advanced Concepts for Nuclear Rocket Propulsion. NASA SP-20, Dec. 1962, pp. 3-16.

2. Spencer, D. F.: Thermal and Criticality Analysis of the Plasma Core Reactor. JPL TR 32-189, Jet Prop. Lab., C.I.T., Jan. 1962.

3. Meghreblian, Robert V.: Thermal Radiation in Gaseous Fission Reactors for Propulsion. JPL TR 32-139, Jet Prop. Lab., C.I.T., July 24, 1961.

4. Lanzo, Chester D., and Ragsdale, Robert G.: Experimental Determination of Spectral and Total Transmissivities of Clouds of Small Particles. NASA TN D-1405, 1962.

5. Wahl, B. W., Gould, R. J., and McKee, J. W.: Radiative Properties of Hydrogen and Radiative Transfer to the Environment at Elevated Temperatures. Eng. Paper 1149, Douglas Aircraft Co., Inc., Aug. 1961.

6. Patch, Richard W.: Methods for Calculating Radiant Heat Transfer in High Temperature Hydrogen Gas. Rep. M-1492-1, United Aircraft Corp., Nov. 1961.

7. Einstein, Thomas H.: Radiant Heat Transfer to Absorbing Gases Enclosed in a Circular Pipe with Conduction, Gas Flow, and Internal Heat Generation. NASA TR R-156, 1963.

8. Weinstein, Herbert, and Todd, Carroll A.: A Numerical Solution of the Problem of Mixing of Laminar Coaxial Streams of Greatly Different Densities - Isothermal Case. NASA TN D-1534, 1963.

9. Siegel, Robert: Transient Heat Transfer for Laminar Slug Flow in Ducts. Jour. Appl. Mech. (Trans. ASME), ser. E, vol. 26, no. 1, Mar. 1959, pp. 140-142.

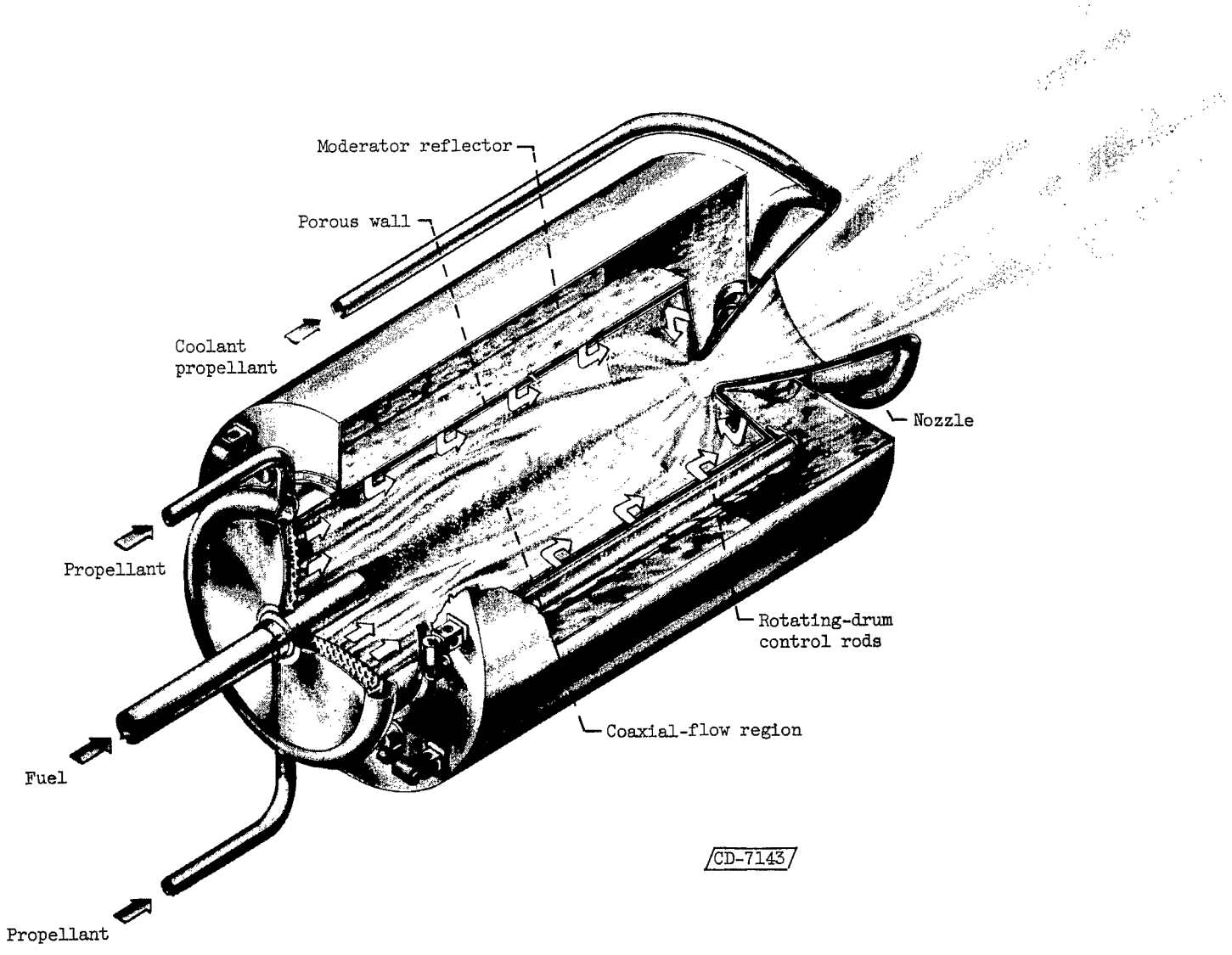

(a) Conceptual illustration.

Figure 1. - Coaxial-flow gaseous reactor.

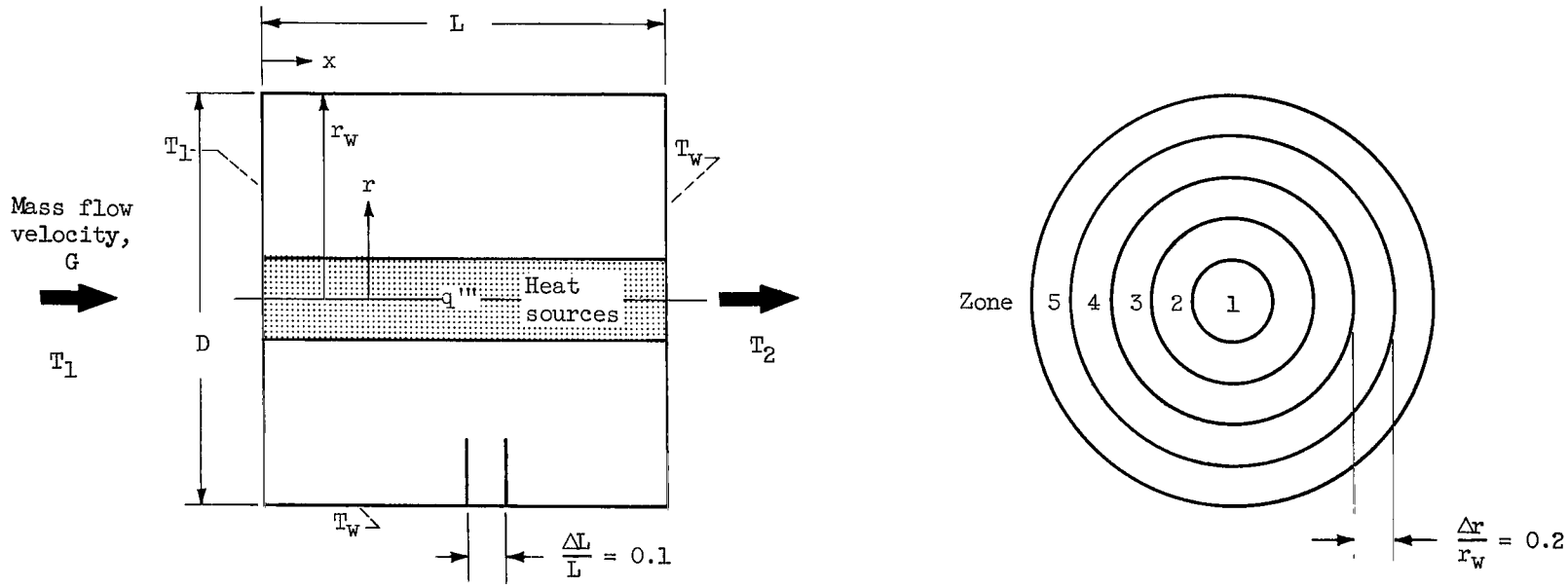

(b) Analytical model.

Figure 1. - Concluded. Coaxial-flow gaseous reactor.

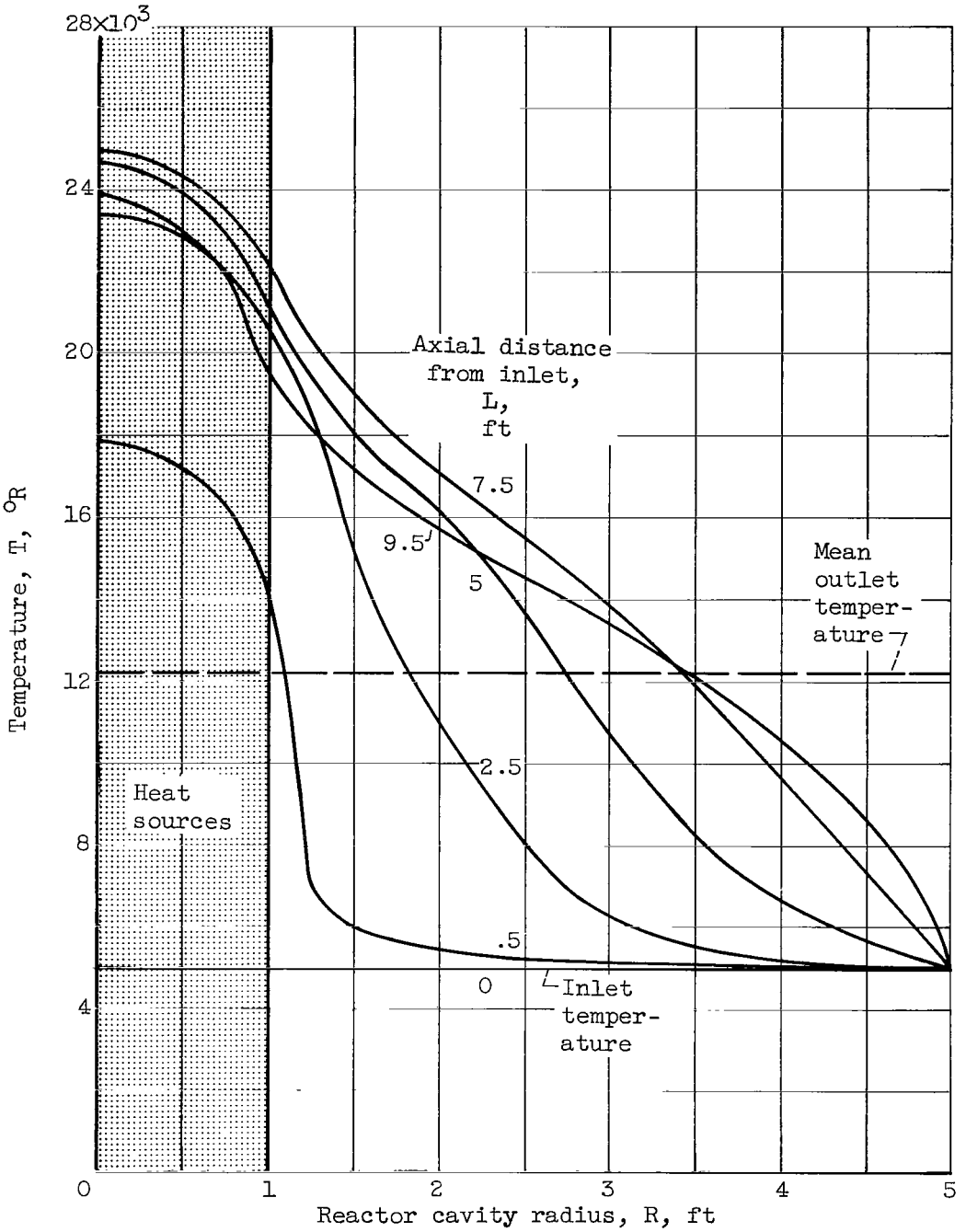

(a) Radial profiles.

Figure 2. - Temperature profiles for illustrative case. Total heat-generation rate, 4.2×10^6 Btu per second; absorption coefficient, 1.4 per foot; propellant flow rate, 33 pounds per second; propellant- to fuel-flow-rate ratio, 24; reactor cavity length, 10 feet; wall temperature, 5000° R.

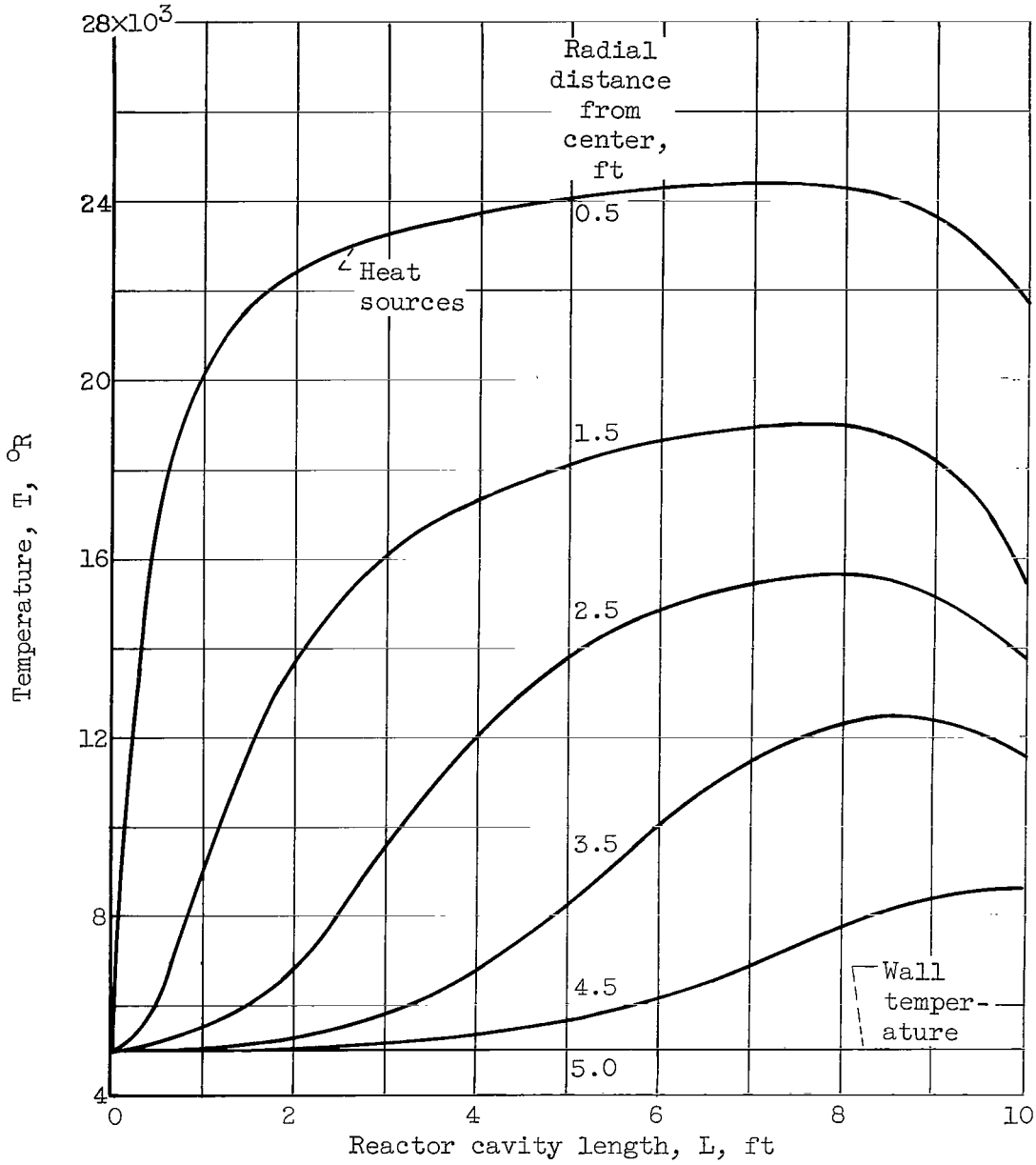

(b) Axial profiles.

Figure 2. - Temperature profiles for illustrative case. Total heat-generation rate, 4.2×10^6 Btu per second; absorption coefficient, 1.4 per foot; propellant flow rate, 33 pounds per second; propellant- to fuel-flow-rate ratio, 24; reactor cavity length, 10 feet; wall temperature, 5000° R.

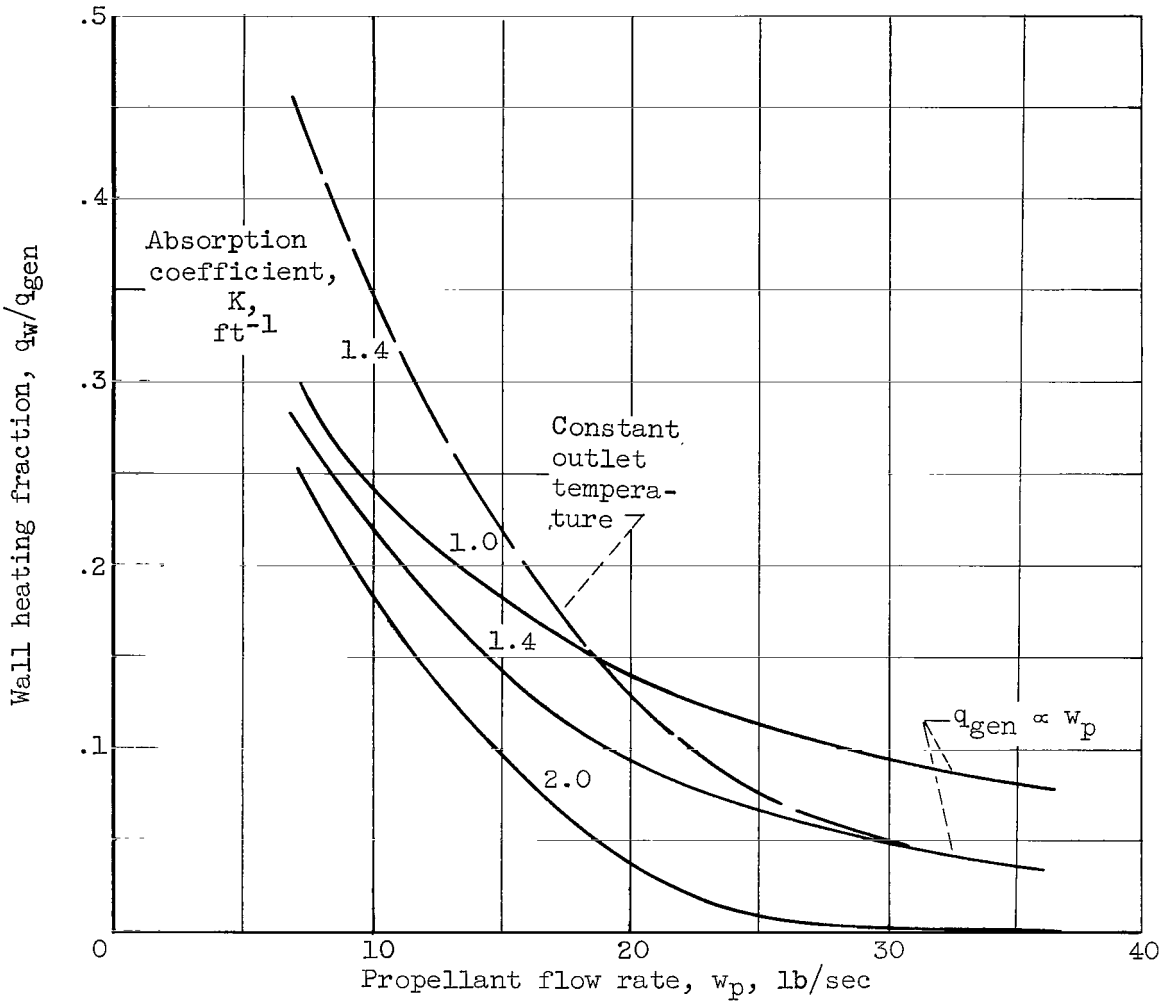

Figure 3. - Effect of propellant flow rate and absorption coefficient on wall heating fraction. Propellant- to fuel-flow-rate ratio, 24; reactor cavity length, 10 feet; reactor cavity radius, 5 feet; inlet and wall temperatures, 5000° R.

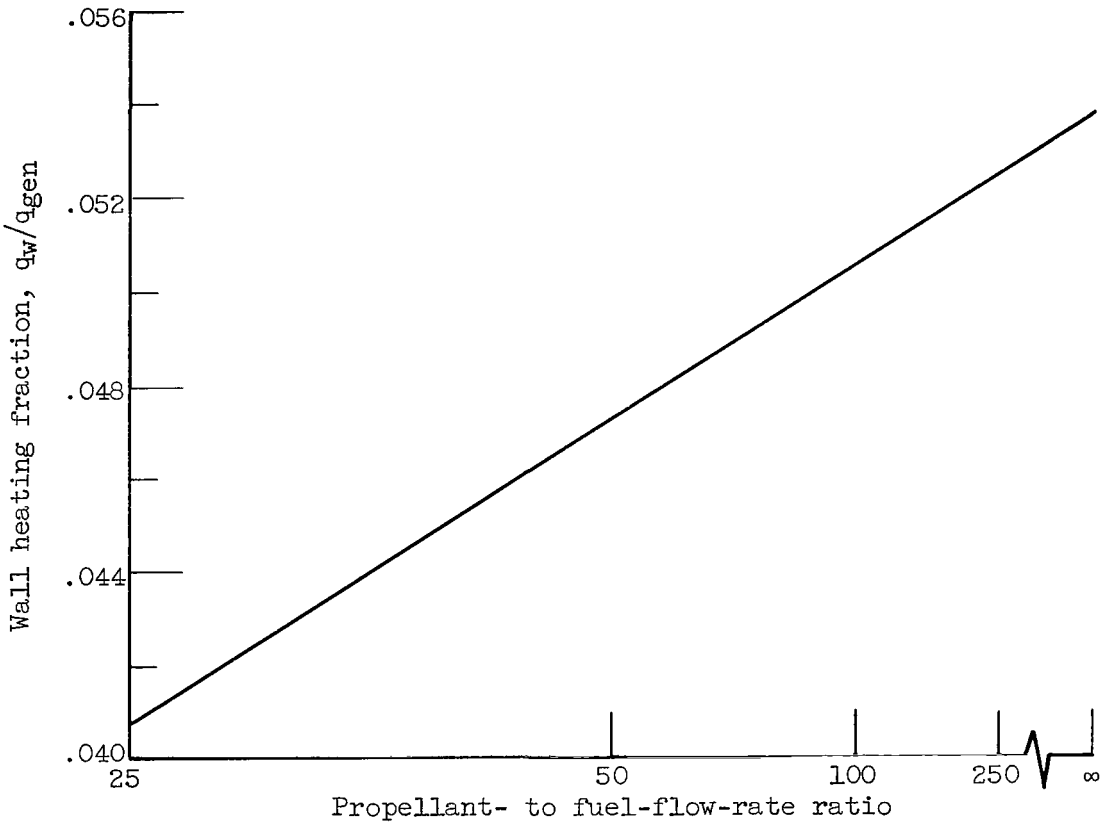

Figure 4. - Effect of propellant- to fuel-flow-rate ratio on wall heating fraction. Total heat-generation rate, 4.2×10^6 Btu per second; absorption coefficient, 1.4 per foot; propellant flow rate, 33 pounds per second; inlet and wall temperatures, 5000° R.

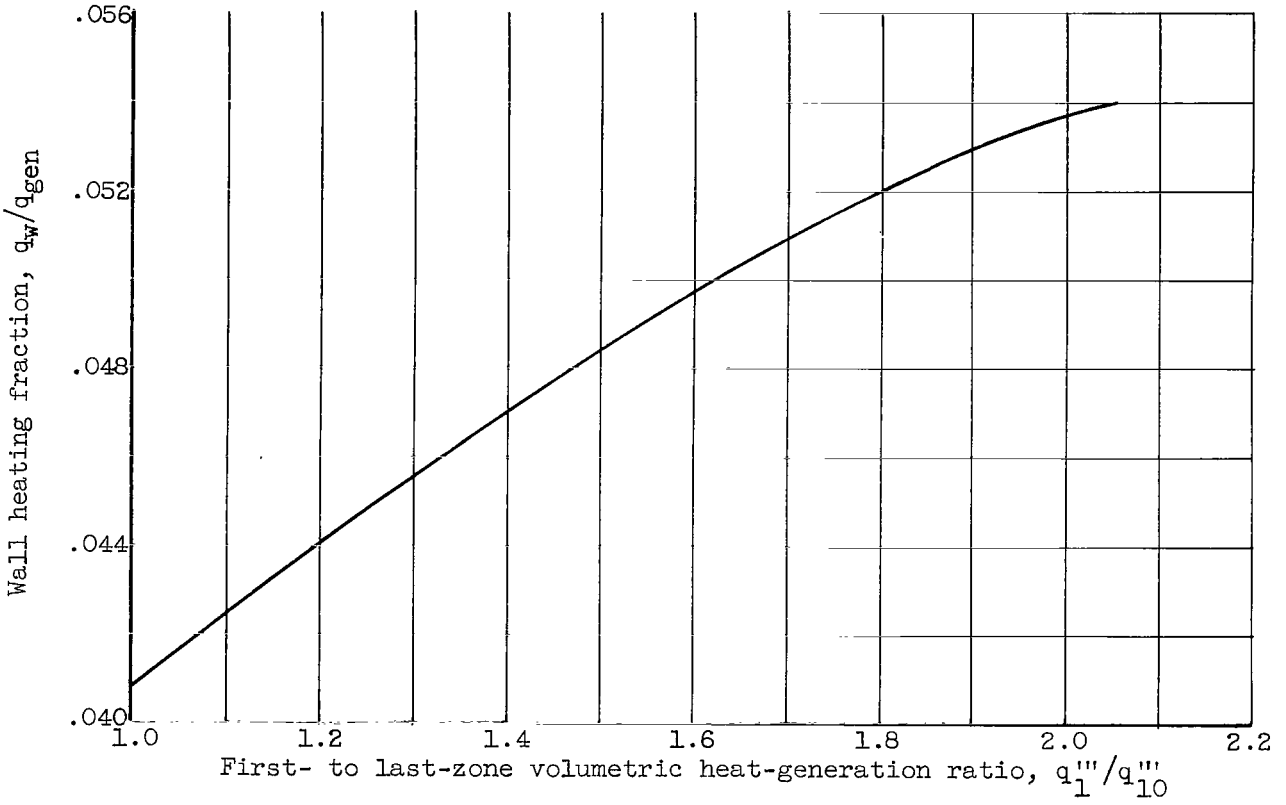

Figure 5. - Effect of linear axial decrease of volumetric heat generation on wall heating fraction. Total heat-generation rate, 4.2×10^6 Btu per second; absorption coefficient, 1.4 per foot; propellant flow rate, 33 pounds per second; propellant- to fuel-flow-rate ratio, 24; reactor cavity length, 10 feet; reactor cavity radius, 5 feet; inlet and wall temperatures, 5000° R.

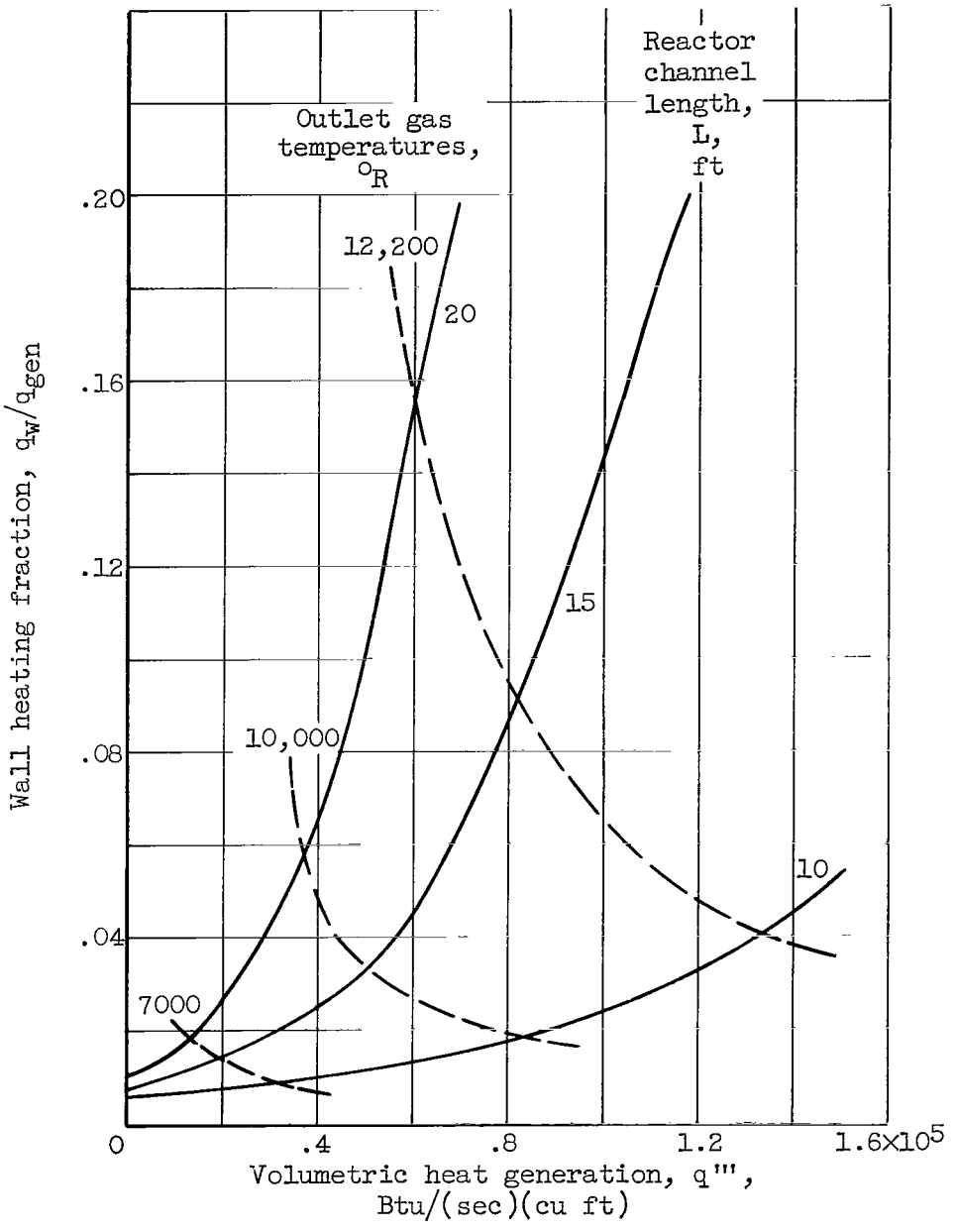

Figure 6. - Effect of volumetric heat-generation rate and reactor cavity length on wall heating fraction. Absorption coefficient, 1.4 per foot; propellant- to fuel-flow-rate ratio, 24; reactor cavity length, 10 feet; reactor cavity radius, 5 feet; inlet and wall temperatures, 5000° R.

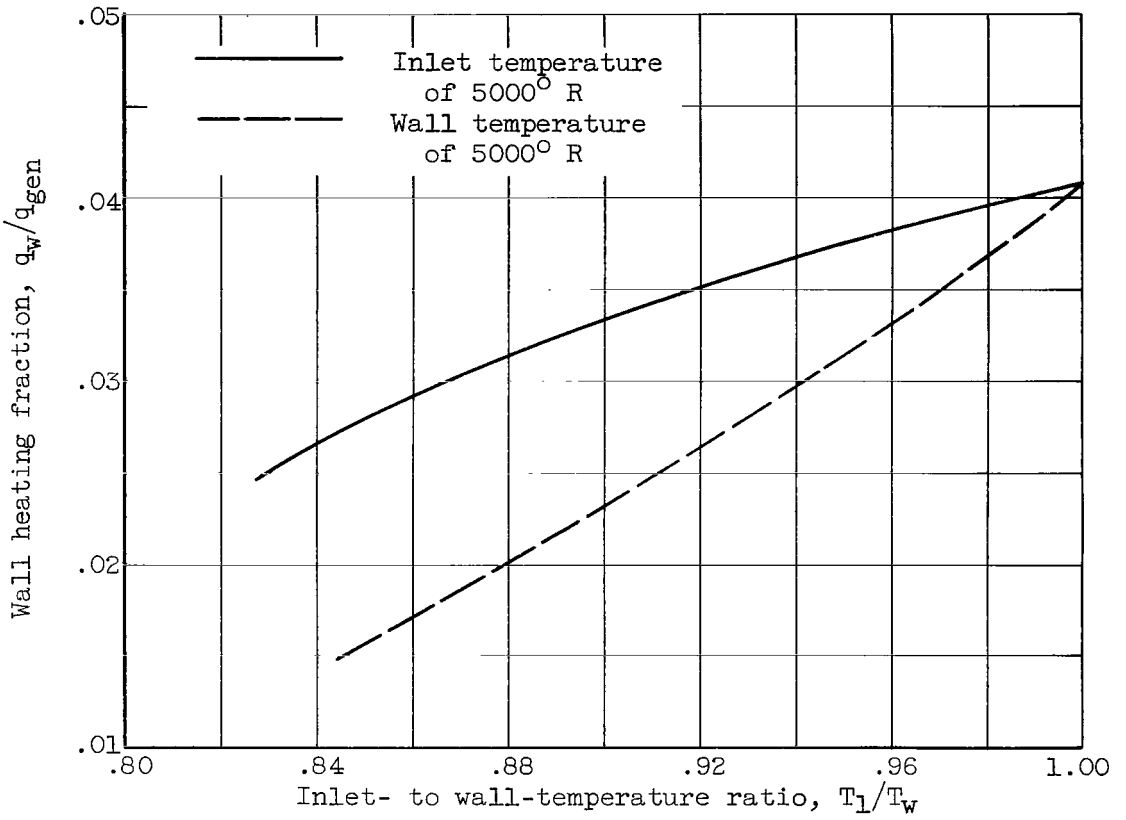

Figure 7. - Effect of inlet- to wall-temperature ratio on wall heating fraction. Total heat-generation rate, 4.2×10^6 Btu per second; absorption coefficient, 1.4 per foot; propellant flow rate, 33 pounds per second; propellant- to fuel-flow-rate ratio, 24; reactor cavity length, 10 feet; reactor cavity radius, 5 feet.

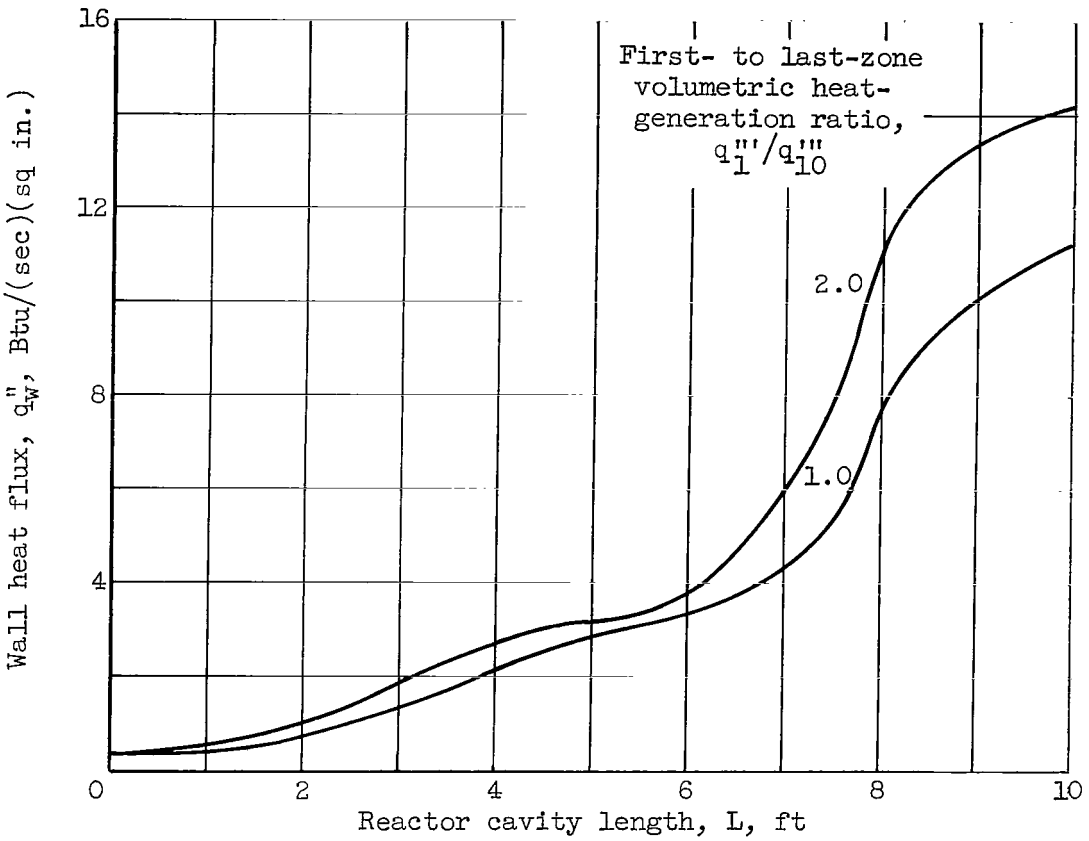

Figure 8. - Axial variation of wall heat flux. Total heat-generation rate, 4.2×10^6 Btu per second; absorption coefficient, 1.4 per foot; propellant flow rate, 33 pounds per second; propellant- to fuel-flow-rate ratio, 24; reactor cavity length, 10 feet; reactor cavity radius, 5 feet; inlet and wall temperatures, 5000° R.

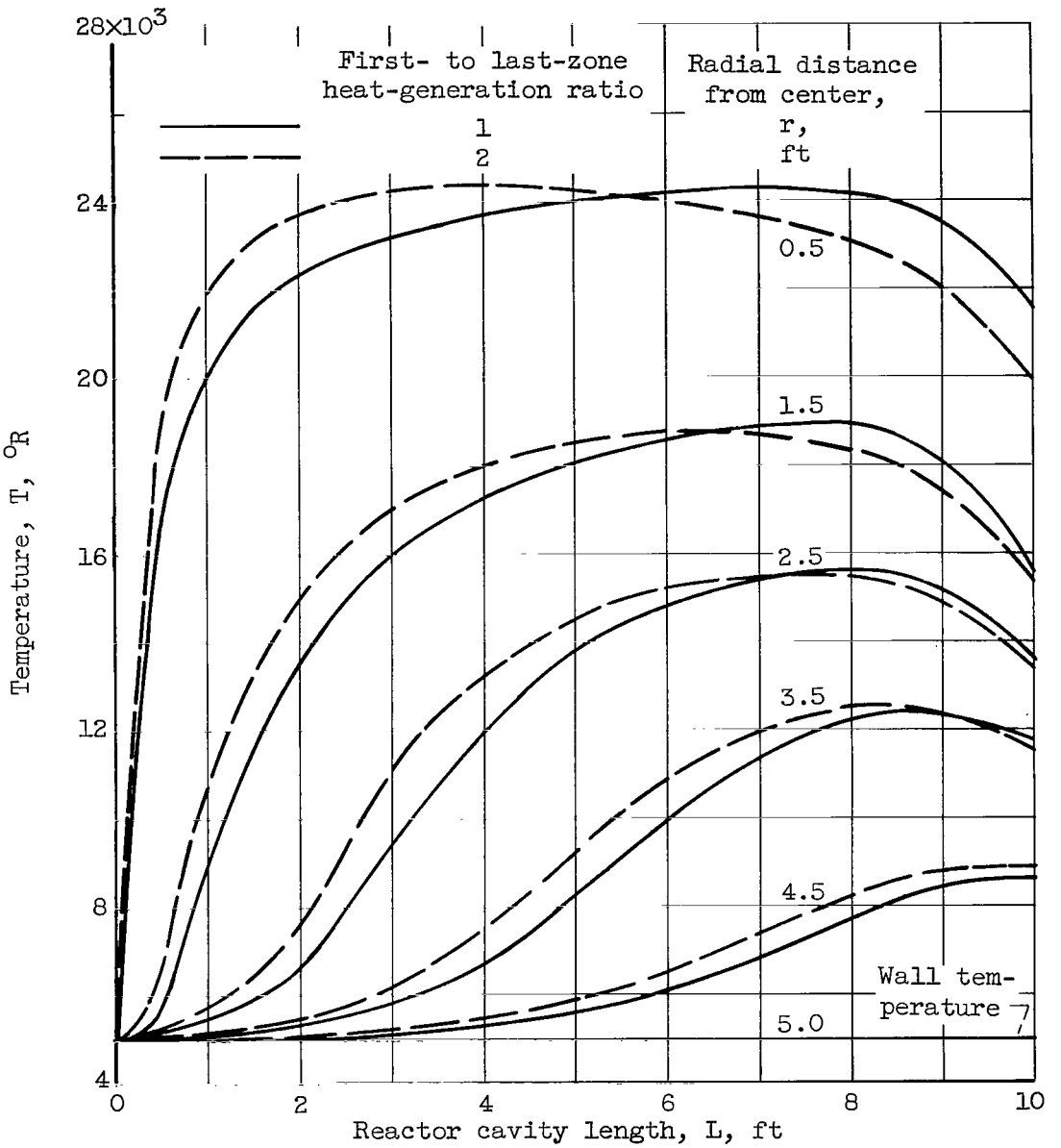

Figure 9. - Effect of axially decreasing volumetric heat-generation rate on axial temperature profiles. Total heat-generation rate, 4.2×10^6 Btu per second; absorption coefficient, 1.4 per foot; propellant flow rate, 33 pounds per second; propellant- to fuel-flow-rate ratio, 24; reactor cavity radius, 5 feet; inlet and wall temperatures, 5000° R.

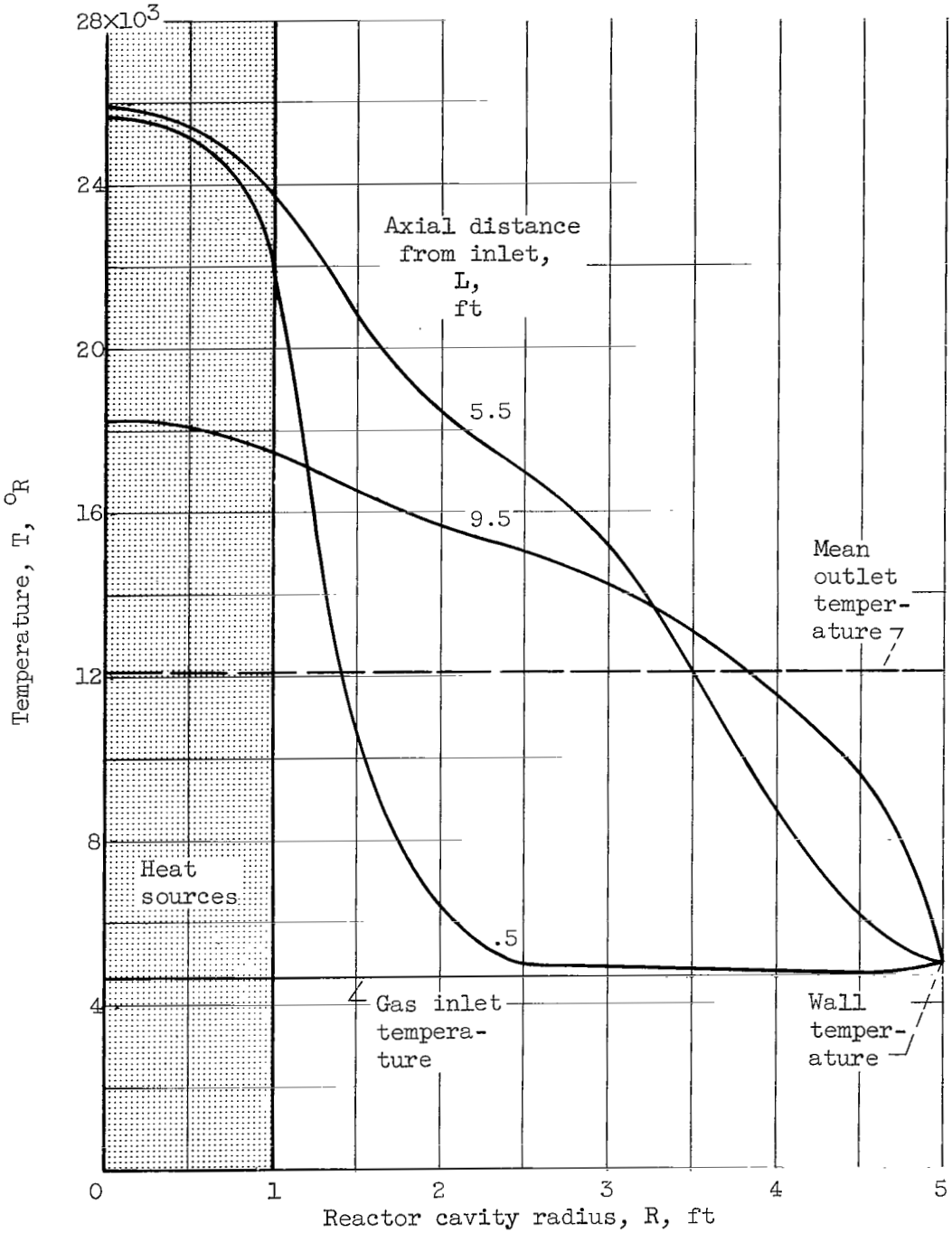

Figure 10. - Temperature profiles for combined gaseous-reactor operating conditions. Total heat-generation rate, 3.9×10^6 Btu per second; absorption coefficient, 2.0 per foot; propellant flow rate, 33 pounds per second; propellant-to fuel-flow rate ratio, 2400; reactor cavity length, 10 feet; first- to last-zone heat-generation ratio, 10.

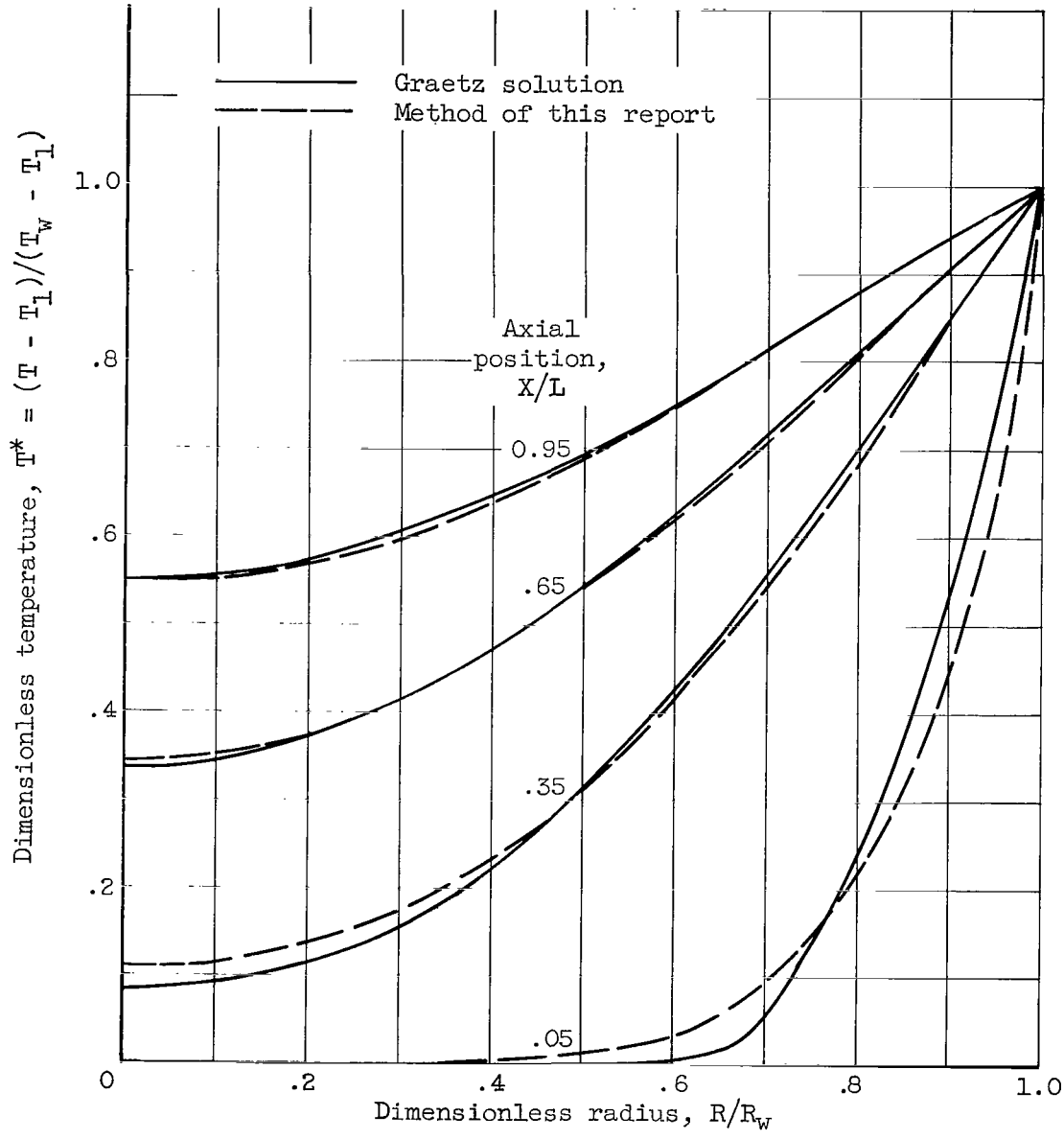

Figure 11. - Comparison of profiles predicted by method of this report with Graetz temperature profiles for laminar slug flow and constant wall temperature: $RePr/(L/D) = 17.5$.